JOURNAL OF MAGNETIC RESONANCE 73, 99–113 (1987)

Broadband Heteronuclear Decoupling in the Presence of Homonuclear Dipolar and Quadrupolar Interactions

K. V. SCHENKER, D. SUTER, AND A. PINES

Department of Chemistry, University of California, and Materials and Molecular Research Division, Lawrence Berkeley Laboratory, Berkeley, California 94720

Received November 12, 1986

A new family of composite decoupling sequences designed for heteronuclear broadband decoupling of spin-1 and spin-$\frac{1}{2}$ in solids and liquid crystals is introduced. The pulse sequences are windowless and perform net rotations in spin space about magic-angle axes. Computer simulations and experimental results are presented to demonstrate their decoupling performance and to discuss their susceptibility toward pulse imperfections. We describe the evaluation of the new sequences, called COMARO (*co*mposite *ma*gic-*a*ngle *ro*tation), and point out some possibilities for further improvements. © 1987 Academic Press, Inc.

INTRODUCTION

The technique of heteronuclear decoupling in NMR has witnessed dramatic improvements in recent years. The former standard technique of noise decoupling has been replaced by composite pulse decoupling with sequences known as MLEV (*1–4*), WALTZ (*5–7*), and others (*7–10*). These broadband decoupling sequences have been designed specifically for isotropic liquids. In oriented systems such as liquid crystals and solids the performance of these decoupling sequences is severely degraded when large dipole–dipole and quadrupolar interactions occur together with even small resonance offsets. This problem has been addressed by Fung *et al.*, investigating the performance of many decoupling sequences for liquid crystal samples (*11–13*). They proposed a family of sequences, applicable to anisotropic spin-$\frac{1}{2}$ systems. The performance of these decoupling sequences and those commonly used for decoupling in isotropic samples is, however, far from satisfactory for many applications in solid-state and liquid crystal NMR, where the decoupling field must overcome not only the heteronuclear couplings but also homonuclear dipolar and quadrupolar interactions.

It has been shown (*14–18*) that it is possible to decouple spins $I = 1$, in particular deuterons, by irradiating the forbidden double-quantum transition which, to first order, is not affected by the quadrupole coupling. However, the effective rf field strength acting on the double-quantum transition is scaled by a factor of ω_1/ω_Q. As a consequence of the weaker rf field strength, the decoupling performance becomes strongly offset dependent. This may not be a severe problem in solid-state spectroscopy where broadening due to residual heteronuclear couplings is masked by other line broadening effects, or if only one type of I spin is present which can be irradiated on resonance. In typical liquid crystal spectroscopy with partially deuterated samples, containing

0022-2364/87 $3.00
Copyright © 1987 by Academic Press, Inc.
All rights of reproduction in any form reserved.

deuterons with different chemical shifts, quadrupolar and homonuclear dipolar interactions, satisfactory decoupling is hardly achievable without critical sample heating. To illustrate this decoupling problem, Fig. 1 shows a deuterium decoupled proton spectrum of a mixture of hexane-d_{12} isotopomers dissolved in a nematic liquid crystal phase (*19*). Each of the four doublets a, b, c, and d stems from a different hexane-d_{12} isotopomer with a splitting due to the proton–proton dipolar interaction. The imperfect decoupling is obvious, mainly for the doublets b and c which display residual couplings to deuterons.

In this paper we present a new type of pulse sequence for heteronuclear decoupling in oriented systems. The main objective was to obtain acceptable decoupling of spin $I = 1$ over an offset range typical for the chemical-shift range of deuterons in a liquid crystal or solid with a rf field strength ω_1 of the same order of magnitude as the quadrupolar coupling constant ω_Q.

EVALUATION OF DECOUPLING SEQUENCES

The efficiency of a decoupling sequence for a I–S spin-$\frac{1}{2}$ system can be assessed with the theory of modulated decoupling given by Waugh (*20*). Under a number of assumptions it leads to the conclusion that the residual splitting J_{res} of the resonance lines in the S spectrum is related to the unperturbed coupling J by a scaling factor λ:

$$J_{res} = \lambda J = (1/t_r) d\Phi/d\delta^I J, \qquad [1]$$

where Φ is the total rotation angle accumulated by an isolated spin $I = \frac{1}{2}$ during one cycle of the decoupling sequence, δ^I is the resonance offset of the I spin, and t_r is the period of the decoupling sequence. Thus the criterion for good decoupling is that $\Phi(\delta^I)$

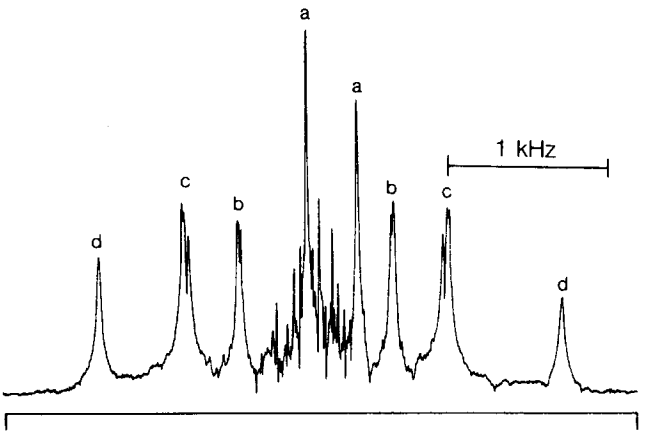

FIG. 1. A cw deuterium-decoupled proton spectrum of a mixture of *n*-hexane-d_{12} isotopomers, dissolved in the liquid crystal phase EK 11650. The irradiation frequency of the deuterium-decoupling field was optimized for a maximum free-induction-decay time. The rf field strength used allowed a maximum acquisition time of 200 ms without excessive sample heating. The full linewidth at half height for the signals (a) is approximately 25 Hz.

changes very little over the desired offset range. The following conditions must be fulfilled if this simple criterion is to apply: the irradiation sequence should be periodic and the decoupling field should be strong compared to the coupling constant.

To analyze the decoupling of a spin $I = 1$ in an oriented system, a somewhat more general formulation of this theory is necessary because in general: (i) the effect of a pulse sequence on a spin $I = 1$ cannot be represented as a simple rotation in three-dimensional space; (ii) the decoupling cannot be described by a single scaling factor. Therefore, instead of the rotation Φ of an isolated spin $I = \frac{1}{2}$, we need to calculate the energy levels E_i^{I} $(i = 1, 2, 3)$ of the average Hamiltonian under a pulse sequence applied to an isolated spin $I = 1$ as a function of the offset δ^{I}. Taking the derivatives of these eigenvalues with respect to the offset δ^{I}, $\partial E_i^{\mathrm{I}}/\partial\delta^{\mathrm{I}}$, is equivalent to $(1/t_r)d\Phi/d\delta^{\mathrm{I}}$ of Eq. [1] for a spin $I = \frac{1}{2}$. The efficiency of a decoupling sequence can therefore easily be analyzed by a computer simulation. Plotting $\partial E_i^{\mathrm{I}}/\partial\delta^{\mathrm{I}}$ versus δ^{I}, one obtains a graph representing the approximate transition frequencies of the three intense lines in the S spectrum.

This approximation holds if the decoupling sequence is periodic, corresponding eigenvectors of the Hamiltonian at the offsets $\delta^{\mathrm{I}} \pm d^{\mathrm{IS}}/2$ (where d^{IS} is the heteronuclear dipolar coupling constant) are approximately parallel, and d^{IS} is sufficiently small. A complete account of this theory appears in the preceding paper (*21*). This approximation not only reduces the dimension of the spin system by a factor of two but also allows the appraisal of a decoupling sequence by looking at a single plot instead of having to analyze spectra calculated for various offsets and coupling constants.

The relevant Hamiltonian for an I–S spin system ($I = 1$, $S = \frac{1}{2}$, S observed) can be written as

$$\mathscr{H} = \mathscr{H}_{\mathrm{O}} + \mathscr{H}_{\mathrm{Q}} + \mathscr{H}_{\mathrm{IS}} = -\delta^{\mathrm{I}} I_{\mathrm{Z}} + \omega_{\mathrm{Q}}(I_{\mathrm{Z}}^2 - 2/3\,\mathbb{1}) + d^{\mathrm{IS}} I_{\mathrm{Z}} S_{\mathrm{Z}}, \qquad [2]$$

where δ^{I} is the resonance offset, ω_{Q} the quadrupole coupling constant, and d^{IS} the heteronuclear coupling constant. Our first approach to the decoupling problem was to find a pulse sequence that would make the zero-order average Hamiltonians (*22*) of all three terms in Eq. [2] vanish. Rules for accomplishing this by fully windowless sequences of $\pi/2$ pulses have been given by Burum *et al.* (*23*). According to these rules, twelve $\pi/2$ pulses are required to fulfill the conditions $\bar{\mathscr{H}}_{\mathrm{O}}^{(0)} = \bar{\mathscr{H}}_{\mathrm{Q}}^{(0)} = \bar{\mathscr{H}}_{\mathrm{IS}}^{(0)} = 0$. Sixteen 12-pulse sequences were analyzed and most of these basic sequences were expanded to 24-, 48-, and some to 96-pulse sequences using symmetrization schemes. Different subclasses of the basic sequences are distinguishable but all have in common that they can be divided into three 4-pulse elements each of which performs either a $\pm 120°$ overall rotation about one of the four cube diagonal axes or a 180 or 360° rotation about the x or y axis in spin space.

Parameters selected for the evaluation of the decoupling performance were $\omega_{\mathrm{Q}} = \omega_1$, where ω_1 is the rf field strength, and $-0.25\,\omega_1 \leqslant \delta^{\mathrm{I}} \leqslant +0.25\,\omega_1$. Although the sequences provided considerable improvement of the decoupling performance over the cw technique, they were clearly not satisfactory. The zero-order average Hamiltonian approach used to derive these sequences is obviously insufficient in this case. This is not surprising since $\mathscr{H}_{\mathrm{Q}}$ is, for $\omega_{\mathrm{Q}} = \omega_1$, far more than a small perturbation of the total Hamiltonian and thus slow or even no convergence of the Magnus expansion may be expected (*22*).

A second approach was to consider shorter pulse sequences which perform overall rotations only about cube diagonal axes in spin space. A short sequence with this behavior consists of two $\pi/2$ pulses with a rf phase difference of 90°. The rotation axis can lie in any of the eight octants of the three-dimensional coordinate system, depending on the rf phases of the $\pi/2$ pulses. The eight possible combinations are given in Table 1.

The decoupling performance of the simple sequence YX is approximately the same as with cw decoupling within the offset range $-0.4\ \omega_1 \leqq \delta^I \leqq 0.4\ \omega_1$; for larger offsets, the YX pulse sequence is expected to decouple slightly better. In order to improve the performance of the decoupling sequence we replaced the $\pi/2$ pulses by composite pulses which provide, over a certain range, offset-independent 90° rotations; such a pulse sequence generates an offset-independent net rotation about a cube diagonal axis. The four composite pulses presented in Table 2 were investigated; only composite pulses with 180° phase shifts were considered.

In all simulations the composite pulse 385 $\overline{320}$ 25 proved clearly superior to the other three. This composite pulse was originally derived as an alternative to a constant 90° net rotation (*28, 29*). With this composite element inserted, the two-pulse cycle YX becomes

$$385_{90}\,320_{270}\,25_{90}\,385_{0}\,320_{180}\,25_{0}, \qquad [3]$$

where we recall that the subscripts denote the relative rf phases. The pulse cycle [3] performs an offset-compensated 120° overall rotation about the (1, 1, 1) axis. For the standard test case $\omega_Q = \omega_1$ at an offset $\delta^I = 0.05\ \omega_1$, this decoupling sequence scales the residual splitting of the outer lines of the intense central multiplet in the S spectrum by a factor of 0.0052. The corresponding scaling factor for cw decoupling is 0.214. It is worth noting that the zero-order average Hamiltonian of sequence [3], repeated three times to produce a 360° rotation, does not vanish. The interpretation is that evidently the remaining zero-order terms do not have to vanish as long as they are constant over the desired range of resonance offset.

TABLE 1

The Overall Rotation Axes of the Eight Two-Pulse Elements $(\pi/2)_\phi(\pi/2)_{\phi\pm90°}$

Pulse sequence[a]	Net rotation axis
YX	(1, 1, 1)
$\bar{X}$Y	(−1, 1, 1)
$\bar{Y}\bar{X}$	(−1, −1, 1)
X$\bar{Y}$	(1, −1, 1)
XY	(1, 1, −1)
Y$\bar{X}$	(−1, 1, −1)
$\bar{X}\bar{Y}$	(−1, −1, −1)
$\bar{Y}$X	(1, −1, −1)

[a] X, Y, $\bar{X}$, and $\bar{Y}$ stand for $\pi/2$ pulses with the relative rf phase 0, 90, 180, and 270°, respectively.

TABLE 2

Composite Pulses for Decoupling Sequences

Composite pulse[a]	Reference
(1) 385 $\overline{320}$ 25	(*24*, *25*)
(2) $\overline{114.3}$ 318.6 $\overline{114.3}$	(*26*)
(3) 24 $\overline{152}$ 346 $\overline{152}$ 24	(*26*)
(4) 135 $\overline{90}$ 45	(*27*)

[a] Nominal pulse flip angles are given in degrees; a bar denotes a 180° phase shift.

The performance of this pulse sequence can be improved by combining the cycle [3] with equivalent cycles having a different net rotation axis. Two questions arise: first, how frequently should the rotation axis be changed and second, which rotation axes should be combined. The answers depend on the magnitude of ω_Q and the number of axes which are built into the cycle. From our computer simulations for the I–S spin system with $\omega_Q = \omega_1$ we found it best to combine only the two rotation axes (1, 1, 1) and (1, −1, −1), or equivalent combinations. The rotation axes are changed after each net rotation of 360°. This results in the cycle

$$\mathrm{YXYXYX}\quad \bar{\mathrm{Y}}\mathrm{X}\bar{\mathrm{Y}}\mathrm{X}\bar{\mathrm{Y}}\mathrm{X}, \qquad [4]$$

where now each X, Y, and $\bar{\mathrm{Y}}$ stands for the respective composite pulse 385 $\overline{320}$ 25. If ω_Q is smaller, for example $\omega_Q = 0.5\ \omega_1$ in our simulations, the combination of the four axes (1, 1, 1), (−1, 1, 1), (1, −1, −1), and (−1, −1, −1), again changed after a net rotation of 360°, produced the best results. The corresponding pulse cycle is

$$\mathrm{YXYXYX}\quad \bar{\mathrm{X}}\mathrm{Y}\bar{\mathrm{X}}\mathrm{Y}\bar{\mathrm{X}}\mathrm{Y}\quad \bar{\mathrm{Y}}\mathrm{X}\bar{\mathrm{Y}}\mathrm{X}\bar{\mathrm{Y}}\mathrm{X}\quad \overline{\mathrm{XY}}\,\overline{\mathrm{XY}}\,\overline{\mathrm{XY}}. \qquad [5]$$

The combination of different rotation axes does diminish the average Hamiltonian of the cycle but makes the cycle time t_r longer. Since in the Magnus expansion the m^{th}-order average Hamiltonian term $\bar{\mathscr{H}}^{(m)}$ is proportional to $(t_r)^m$ (*22*), a long t_r emphasizes the higher-order terms. Therefore, a short t_r is important in cases where the Magnus expansion shows slow convergence, e.g., for large ω_Q. If the convergence is good, e.g., for small ω_Q, a longer t_r may be acceptable. The short t_r of the basic cycle [3] is, however, not the key to overcome large ω_Q. Even for $\omega_Q = 2.5\ \omega_1$ better decoupling over a wider offset range is to be expected from sequence [4] because [3] is considerably more susceptible to pulse imperfections than [4]. On the other hand, the combination of more than four rotation axes can improve the decoupling performance for a small ω_Q at the price of a reduced offset range.

We term the basic sequence [3] COMARO (*co*mposite *ma*gic-*a*ngle *ro*tation), the sequences [4] and [5] COMARO-2 and COMARO-4, respectively, where the numbers 2 and 4 refer to the number of net rotation axes combined in the sequence cycle.

QUANTITATIVE DESCRIPTION OF COMARO-2 AND COMARO-4

In this section we compare the decoupling sequences COMARO-2 and COMARO-4 with the cw technique and describe their performance under the assumption of pulse

angle missets (rf inhomogeneity) and rf phase errors. All results are based on computer simulations and all frequencies are given in units of ω_1, the rf field strength. The following section discusses experimental results.

In Fig. 2, a series of COMARO-2 and cw decoupled S spectra are compared for an I–S spin system with spin $I = 1$ and spin $S = \frac{1}{2}$. The quadrupole coupling constant was set to $\omega_Q = \omega_1$, the heteronuclear dipole–dipole coupling constant to $d^{IS} = 0.1$ ω_1, and the full linewidth at half height was assumed to be $\Delta\omega = 0.0002$ ω_1. The offset δ^I was varied from 0 to 0.05 ω_1. To translate these parameters into a practical case, e.g., I ≡ deuteron and S ≡ proton, we can set $\omega_1 = 10{,}000$ Hz giving $\omega_Q = 10{,}000$ Hz, $d^{IS} = 1000$ Hz, $\Delta\omega = 2$ Hz, and 0 Hz $\leq |\delta^I| \leq 500$ Hz. These are typical values for ω_1, ω_Q, and d^{IS} in liquid crystal NMR. The linewidth was chosen as 2 Hz to provide a sensitive indication of imperfect decoupling; it is often larger in experimental liquid crystal NMR spectra. The offset range to be covered depends on the static field strength of the spectrometer. Figure 2 demonstrates the strong susceptibility of the cw decoupling technique to resonance offset. The COMARO-2 sequence, on the other hand, provides satisfactory decoupling over a considerable offset range. The weak satellites in the COMARO-2 spectra correspond to those in the cw decoupled spectra. They show up

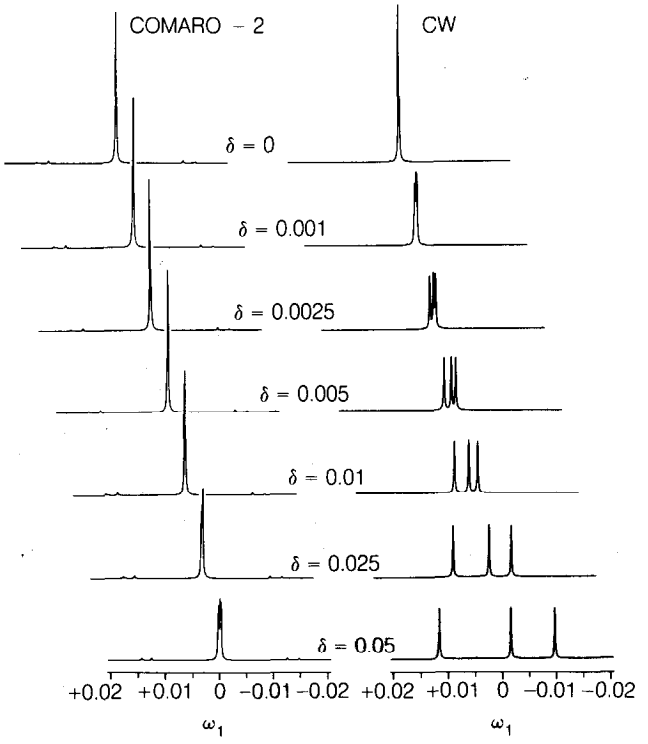

FIG. 2. Calculated COMARO-2 and cw decoupled S spectra. The spin system is an I–S pair (spin $I = 1$, $S = \frac{1}{2}$) with a dipole–dipole coupling constant $d^{IS} = 0.1$ ω_1 and a quadrupole coupling constant for the spin I with $\omega_Q = \omega_1$. The offset is given in units of ω_1. The assumed linewidth $\Delta\omega$ is 0.0002 ω_1.

at different frequency positions and are slightly more intense, but typically less than 3% of the main signal.

An important feature of a decoupling sequence, if it is to be used for oriented systems, is insensitivity to homonuclear dipole–dipole coupling among the spins to be decoupled. Figure 3 shows COMARO-2 decoupled S spectra of a I_2S spin system. The offsets of the two I spins are $\delta_1^I = 0.005\ \omega_1$ and $\delta_2^I = 0.01\ \omega_1$, the quadrupole coupling constants are $\omega_Q(I_1) = \omega_Q(I_2) = \omega_1$, and the heteronuclear dipole coupling constants are $d_1^{IS} = 0.1\ \omega_1$ and $d_2^{IS} = 0.05\ \omega_1$. This example demonstrates that no severe degradation of the decoupling performance is to be expected for $d_{12}^{II} < 0.03\ \omega_1$, a range which appears adequate for most practical applications. In addition we considered scalar homonuclear interactions among the I spins. They were found to cause no problems as long as $J_{12}^{II} < 0.01\ \omega_1$, a limit far higher than that encountered in deuterium decoupling (e.g., $J_{12}^{II} < 100$ Hz for $\omega_1 = 10{,}000$ Hz).

A comparative representation of the decoupling performance of the cw technique, the COMARO-2, and COMARO-4 sequences is given in Fig. 4, again for an I–S spin system with spin $I = 1$ and spin $S = \frac{1}{2}$. The derivatives $\partial E_i^I/\partial\delta^I$ discussed in the preceding section are plotted versus the resonance offset δ^I. The three curves in each plot can be read as the relative position of the three intense lines in the S spectrum as a function of the offset. Their respective frequencies are given by $d^{IS}\ \partial E_i^I/\partial\delta^I$. The vertical line in the top right plot represents the case of the cw decoupled spectrum in the bottom trace of Fig. 2 where $\delta^I = 0.05\ \omega_1$. The three intersection points with the vertical line give the line positions in the S spectrum. The left three plots are calculated for $\omega_Q = 0.5\ \omega_1$, the right three for $\omega_Q = \omega_1$, and the offset is varied in both cases from $-0.5\ \omega_1$ to $+0.5\ \omega_1$. Note that the vertical scale for the COMARO sequences is expanded by a factor of ten.

Comparing the two COMARO sequences, COMARO-2 is superior to COMARO-4 for the case $\omega_Q = \omega_1$. For $\omega_Q = 0.5\ \omega_1$ the COMARO-4 sequence performs slightly better. For smaller ω_Q/ω_1 ratios the decoupling performance improves for both sequences. The main advantage of COMARO-4 over COMARO-2 in this ω_Q region is its smaller susceptibility to reduced rf field strength (typically found in the outer sections

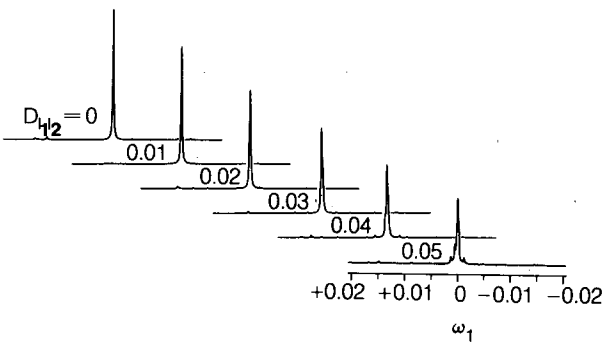

FIG. 3. Calculated COMARO-2 decoupled S spectra for an increasing homonuclear dipole–dipole coupling constant d_{12}^{II} in an I_2S spin system. The d_{12}^{II} values are given in units of ω_1. Coupling constants ω_Q and d^{IS} and offsets δ_1^I and δ_2^I are given in the text.

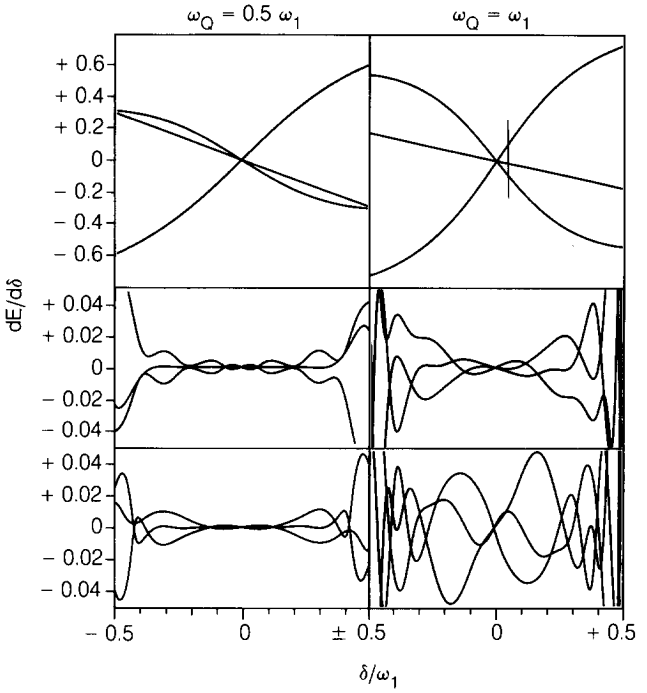

FIG. 4. Plots of $\partial E_1^1/\partial\delta^1$ versus the resonance offset δ^1 for cw (top), COMARO-2 (middle), and COMARO-4 (bottom) decoupling for an I–S spin system for the two situations $\omega_Q = 0.5\ \omega_1$ and $\omega_Q = \omega_1$.

of a decoupler coil), generating pulse angles below the nominal values. At the other end of the ω_Q range, the COMARO-2 sequence can be used up to $\omega_Q = 2.5\ \omega_1$.

In Fig. 5 we present COMARO-4 simulations, once more for the I–S spin system with $\omega_Q = 0.5\ \omega_1$, assuming different pulse angle missets and rf phase errors. The diagrams are equivalent to those shown in Fig. 4. For comparison, plot (a) shows the result obtained with perfect pulses. If one sets all pulse angles of the decoupling sequence to 90% of their nominal values, the curves of plot (b) are obtained. There is almost no degradation of the decoupling performance within the offset range $-0.125\ \omega_1 < \delta^1 < 0.125\ \omega_1$. This insensitivity is significant because spatial inhomogeneity of the rf field strength is normally unavoidable. The COMARO-4 sequence is more sensitive to pulse angles set above the nominal values. Plot (c) shows results obtained assuming pulse angles set to 110% of their nominal values. This is, however, not a severe shortcoming since insensitivity to excessive pulse angles is a relatively unimportant property of a decoupling sequence.

An essential part of composite pulse decoupling is the use of rf phase shifts. In the COMARO sequences the four relative rf phase values 0, 90, 180, and 270° are incorporated. Therefore, phase-shift errors are a potential source of degradation of the decoupling performance. In our simulations we considered two types of phase errors. In both cases two of the four quadrature phase channels are misset by +2°. The result of plot (d) was calculated assuming a misset in the X and Y channel, plot (e) was

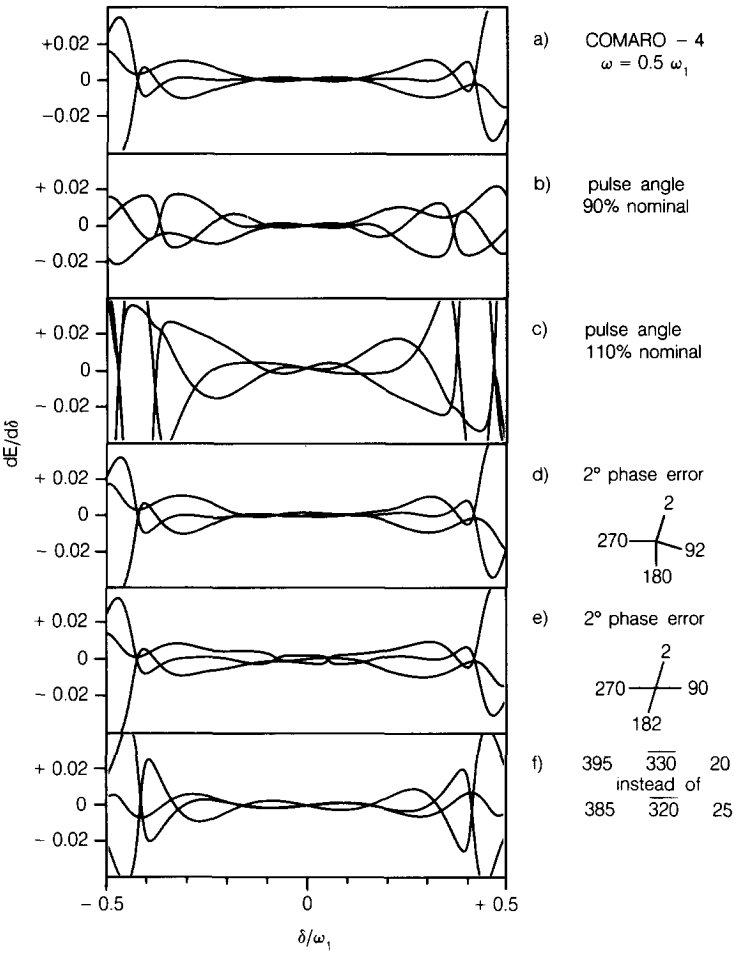

FIG. 5. The decoupling performance of the COMARO-4 sequence under the assumption of different pulse imperfections for an I–S spin system with $\omega_Q = 0.5\ \omega_1$. Plotted are the three derivatives $\partial E_i/\partial\delta^1$ versus the resonance offset δ^1. Perfect pulses were assumed for plot (a), for plots (b) and (c) pulse angles 90 and 110% of the nominal values were assumed, for the calculation of plots (d) and (e) the rf phases in the X and Y channel and X and $\bar{X}$ channel, respectively, were misset by +2°, and for plot (f) a composite element 395 330 20 instead of 385 320 25 was used.

obtained with a misset in the X and $\bar{X}$ channel. COMARO-4 is remarkably insensitive toward the phase errors assumed in case (d). Its behavior under the conditions of case (e) is somewhat inferior, but still satisfactory. The imperfection considered in the case of plot (f) was a pulse angle misset within the basic 90° composite pulse element. Instead of the nominal element 385 $\overline{320}$ 25, these results were calculated with the element 395 $\overline{330}$ 20.

The same calculations were done for the COMARO-2 sequence. The results can be summarized as follows. The most significant difference compared to COMARO-4 is, as already mentioned, the increased susceptibility toward pulse angles smaller than

the nominal values, but to an extent which is still not critical in most applications. For pulse angles above the nominal values the results for COMARO-2 are about the same. An interesting difference between COMARO-2 and COMARO-4 emerges comparing the results for the two phase-error cases (d) and (e). COMARO-2 is somewhat more susceptible toward a misset as assumed in case (d), but clearly less susceptible if the misset occurs in the X and $\bar{X}$ channel (case (e)).

In the introduction we mentioned that decoupling sequences such as MLEV, WALTZ, etc., are not suitable for spin-$\frac{1}{2}$ systems in liquid crystal matrices. In Fig. 6 we demonstrate the decoupling performance of COMARO-4 in such a case. The four derivatives $\partial E_i^I/\partial\delta^I$ of a I_2S spin-$\frac{1}{2}$ system are plotted versus the resonance offset δ^I. Having I = protons in mind, the results were calculated for a homonuclear dipole coupling constant $d_{12}^{II} = 0.5\ \omega_1$ and a shift difference between the two I spins of $\delta_1^I - \delta_2^I = 0.05\ \omega_1$. Earlier in this section we stated that the relative frequencies of the transitions in the S spectrum can be calculated as $d^{IS}\ \partial E_i^I/\partial\delta^I$. For more than one I spin, this holds only if the heteronuclear coupling constants are equal: $d_1^{IS} = d_2^{IS}$(21).

The offset range over which good decoupling is attainable with COMARO-4 is roughly $-0.35\ \omega_1 < \delta^I < 0.35\ \omega_1$, more or less independent of the magnitude of d_{12}^{II}. The decoupling performance is, however, better for smaller d_{12}^{II}. This offset range is a factor of three smaller than what one gets with, e.g., WALTZ-16 in isotropic liquids. This is the price paid for overcoming the additional interactions. In Fig. 7 we compare five calculated spectra decoupled with COMARO-4, WALTZ-16, MLEV-16, cw, and ALPHA-26. The I_3S spin-$\frac{1}{2}$ system and the decoupling field strength were the same for all decoupling methods. The shift and coupling parameters are, all in units of ω_1: $\delta_1^I = 0.005$, $\delta_2^I = 0.01$, $\delta_3^I = 0.02$, $d_{12}^{II} = 0.05$, $d_{13}^{II} = 0.1$, $d_{23}^{II} = 0.15$, $d_1^{IS} = 0.2$, $d_2^{IS} = 0.1$, and $d_3^{IS} = 0.1$. This figure confirms the potential applicability of COMARO-4 to spin decoupling in oriented molecules with homonuclear dipole–dipole interactions.

EXPERIMENTAL RESULTS

The COMARO-2 and COMARO-4 decoupling sequences were tested experimentally by studying the deuterium-decoupled proton spectrum of dimethoxybenzene-d_8. The

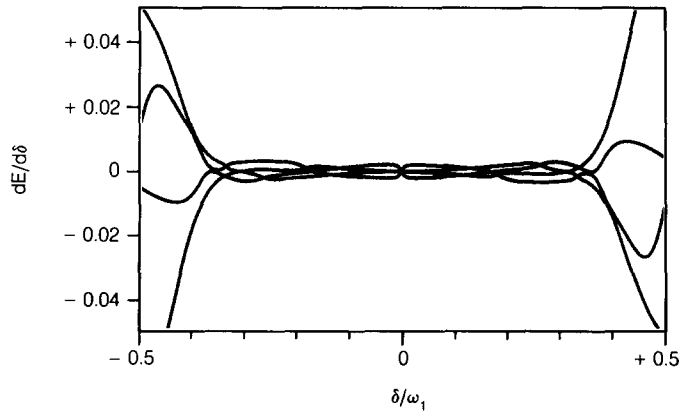

FIG. 6. The four $\partial E_i/\partial\delta^I$ derivatives for an I_2S spin system (spin $I = S = \frac{1}{2}$) versus the resonance offset δ^I. The four curves give the signal frequencies in the S spectrum for the case $d_1^{IS} = d_2^{IS}$.

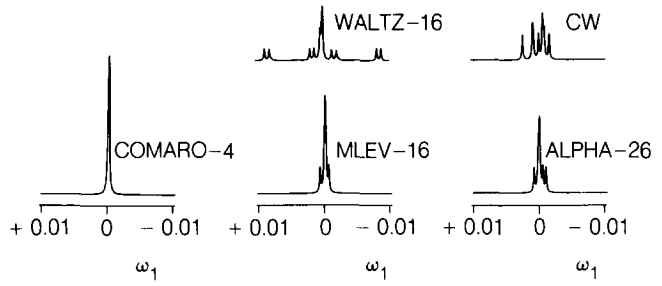

FIG. 7. The calculated S spectra of an I_3S spin system (spin $I = S = \frac{1}{2}$) decoupled with COMARO-4, WALTZ-16, MLEV-16, cw, and ALPHA-26. The signal intensities of all plots are directly comparable.

two methoxy groups each have one proton; the rest of the proton positions were deuterated. The dimethoxybenzene was dissolved in the nematic liquid crystal phase EK 11650 with a concentration of 32 mol%. The sample was in a standard 5 mm tube with a filling height of 45 mm. The sample tube was spun at a rate of approximately 40 Hz. The spectra were measured on a home-built 360 MHz spectrometer at 28°C. The rf field strength in the deuterium-decoupling channel was set to 4035 Hz. The pulse sequence was programmed on a home-built pulse programmer. The ^{1}H FID acquisition was synchronized with the decoupler cycling, sampling 12 and 24 times per cycle in the COMARO-2 and COMARO-4 sequence, respectively. The complex FID points were sampled at the beginning of the 385° pulses in each 385 $\overline{320}$ 25 composite element, giving a spectral width of 1990 Hz. No significant delays between the rf pulses occurred. The proton spectra were measured with a $\pi/2$ pulse excitation followed immediately by the acquisition of the FID. This gave a minor baseline distortion due to the broad signal of the liquid crystal solvent.

In Fig. 8 we present the deuterium spectrum of dimethoxybenzene-d_8 to give the reader an idea of the decoupling problem. The two intense outer peaks are assigned to the methoxy deuterons with an $\omega_Q \approx 1060$ Hz. The inner multiplet of the ring deuterons was not analyzed in detail, but from the separation of the two symmetric

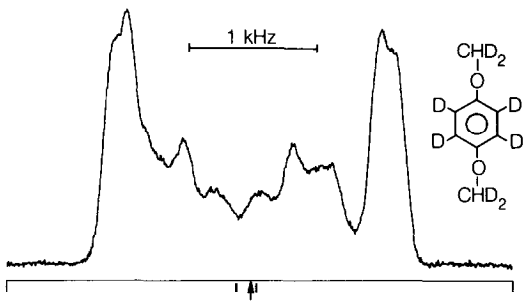

FIG. 8. Experimental deuterium spectrum of dimethoxybenzene-d_8, dissolved in the nematic phase EK 11650. This sample was used to obtain the experimental results presented in Figs. 9–11. The two markers indicate that Larmor frequencies of the two nonequivalent deuterons and the arrow indicates the reference value for the offset δ^1 in Figs. 9 and 11.

parts an $\omega_Q \approx 440$ Hz can be assumed for these deuterons. The chemical-shift difference between the methoxy and the ring deuterons is approximately 128 Hz. The two markers on the frequency axes indicate the chemical shift of the ring and methoxy deuterons, respectively, and the arrow marks the deuteron irradiation position giving the best cw decoupled proton spectrum of dimethoxybenzene-d_8.

Our test sample gave a deuterium-decoupled proton spectrum showing a doublet split by 312 Hz, corresponding to a dipole–dipole coupling constant for the two protons of $d^{HH} = 208$ Hz. In all subsequent figures only the high-field signal of this doublet is reproduced. In Fig. 9 we compare the cw decoupling technique with COMARO-2 and COMARO-4. The proton resonance is shown as a function of the deuterium resonance offset, incremented in 100 Hz steps. The signals shown were obtained by Fourier transformation of a single-shot FID without applying any filter function. The full linewidths at half height at 0 Hz offset are 7.8 Hz for the cw decoupled signal, 3.4 Hz for the COMARO-2 decoupled signal, and 3.6 Hz for the COMARO-4 decoupled signal. The reason for the broadened cw decoupled signal is that the two types of deuterons have different chemical shift, so that the decoupling is not on resonance for either of them. The two arrows on the offset axis mark the resonance frequencies of the ring and methoxy deuterons, respectively. The slight asymmetry with respect to the offset sign is believed to be due to the asymmetry of the spin system. The decoupling performance of COMARO-4 is slightly reduced compared to COMARO-2. A possible explanation is that there are rf phase errors in the X and $\bar{X}$ channel (cf. Fig. 5e) toward which COMARO-4 is more susceptible than COMARO-2. The effective bandwidth is approximately $0.5\omega_1$, in agreement with the computer simulations.

In Fig. 10 COMARO-4 decoupled proton signals are shown which were obtained with deliberately misset pulse lengths. The signal at 100% was measured with pulse

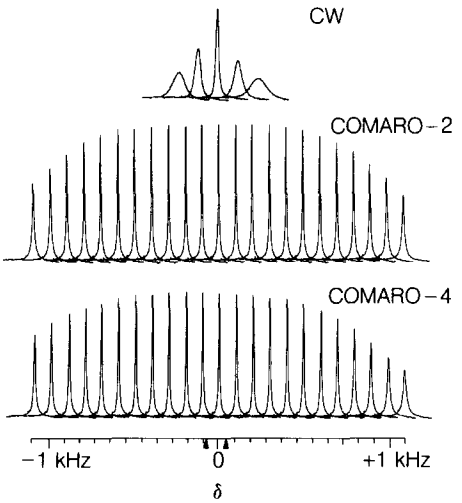

FIG. 9. Experimental proton signals from dimethoxybenzene-d_8, decoupled with cw irradiation, COMARO-2, and COMARO-4 as a function of the deuterium resonance offset. The zero-frequency offset $\delta^I = 0$ Hz corresponds to the deuteron frequency giving the best cw decoupling and is indicated by an arrow in Fig. 8.

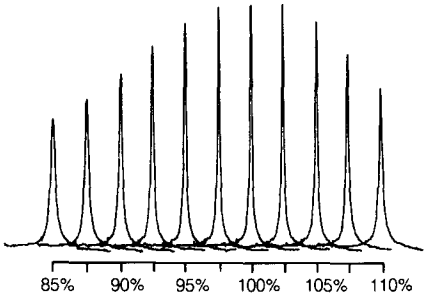

FIG. 10. Experimental proton spectra of dimethoxybenzene-d_8, decoupled with the COMARO-4 sequence, are shown. The pulse angles of all pulses were set to a value between 85 and 110% of their nominal pulse angles. The deuterium resonance offset was $\delta^1 = 0$ Hz.

lengths calculated assuming a rf field strength of 4035 Hz. The pulse lengths were incremented in steps of 2.5% from 85 to 110%. The deuterium offset was 0 Hz. For the signals shown in Fig. 11, the pulse lengths were set to 105% and the deuterium offset was incremented in 300 Hz steps. According to the results presented in Figs. 5b and 5c, the COMARO-4 sequence is less susceptible toward pulse-angle missets below the nominal values. Indeed, Figs. 10 and 11 demonstrate the insensitivity of COMARO-4 to pulse-angle missets or rf inhomogeneities.

CONCLUSIONS

Composite pulse decoupling sequences have proved useful for heteronuclear broadband decoupling in isotropic liquids. In this paper a family of such sequences for decoupling in oriented systems was introduced. The main task was to attain satisfactory decoupling with minimum rf field strength over an offset range typical for protons and deuterons in the presence of strong homonuclear dipole–dipole and quadrupole couplings. The COMARO sequences provide such decoupling and were demonstrated experimentally.

The strategy of decoupling sequences such as MLEV and WALTZ is based on a composite pulse element providing broadband inversion of z magnetization. An ex-

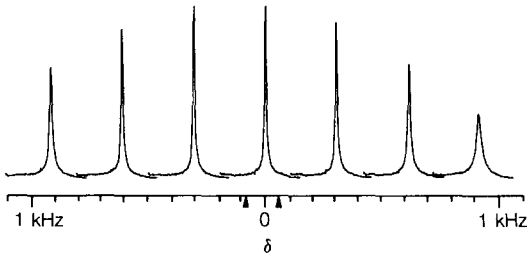

FIG. 11. Experimental proton signals from dimethoxybenzene-d_8, decoupled with the COMARO-4 sequence, are shown as a function of the deuterium resonance offset δ^1. All pulse angles were set to 105% of their nominal values.

pansion procedure is applied to this basic inversion element in order to improve the performance of the decoupling sequence. These procedures have been analyzed and described in detail (*4, 7, 30*), allowing a consistent design of such sequences. The starting point for the COMARO sequences is a composite pulse element performing a rotation about a magic-angle axis. In our approach we used for this purpose two composite $\pi/2$ pulses with 90° phase-shifted net rotation axes. There are certainly different ways to attain this goal leaving room for improvements. One possibility is to develop and explore the use of other composite $\pi/2$ pulses designed especially for this purpose. In particular one may drop the restriction that the composite element performing the magic-angle rotation is decomposable into two equivalent elements as is the case for the basic COMARO sequence [3]. This property of the sequence [3] is not critical.

The combination of different magic-angle rotation axes, changed after a net rotation of 360°, is one possible expansion scheme applicable to this basic element. The particular choice of the rotation axes in COMARO-2 and COMARO-4 is based on numerical results from computer simulations. This expansion procedure is only one of a number of potentially useful expansion schemes applicable to sequence [3]. New composite elements replacing sequence [3] may expand the possibilities for iterative procedures. A detailed analysis of such possibilities should facilitate the design of offspring of the COMARO family.

ACKNOWLEDGMENTS

We gratefully acknowledge helpful discussions with A. J. Shaka. This work was supported by the Director, Office of Energy Research, Office of Basic Energy Sciences, Materials Sciences Division of the U.S. Department of Energy under Contract DE-AC03-76SF00098. K.V.S. acknowledges support by the Swiss National Science Foundation.

REFERENCES

1. M. H. LEVITT AND R. FREEMAN, *J. Magn. Reson.* **43,** 502 (1981).
2. M. H. LEVITT, R. FREEMAN, AND T. FRENKIEL, *J. Magn. Reson.* **47,** 328 (1982).
3. M. H. LEVITT, R. FREEMAN, AND T. FRENKIEL, *J. Magn. Reson.* **50,** 157 (1982).
4. M. H. LEVITT, R. FREEMAN, AND T. FRENKIEL, *in* "Advances in Magnetic Resonance" (J. S. Waugh, Ed.), Vol. 11, p. 47, Academic Press, New York, 1983.
5. A. J. SHAKA, J. KEELER, T. FRENKIEL, AND R. FREEMAN, *J. Magn. Reson.* **52,** 335 (1983).
6. A. J. SHAKA, J. KEELER, AND R. FREEMAN, *J. Magn. Reson.* **53,** 313 (1983).
7. A. J. SHAKA AND J. KEELER, *Prog. NMR Spectrosc.* **19,** 47 (1986).
8. B. M. FUNG, *J. Magn. Reson.* **59,** 275 (1984).
9. B. M. FUNG, *J. Magn. Reson.* **60,** 424 (1984).
10. A. J. SHAKA, P. B. BARKER, AND R. FREEMAN, *J. Magn. Reson.* **64,** 547 (1985).
11. B. M. FUNG, D. S. L. MUI, I. R. BONNELL, AND E. L. ENWALL, *J. Magn. Reson.* **58,** 254 (1984).
12. B. M. FUNG AND P. PARHAMI, *J. Magn. Reson.* **63,** 168 (1985).
13. D. L. MUI, B. M. FUNG, I. R. BONNELL, AND E. L. ENWALL, *J. Magn. Reson.* **64,** 124 (1985).
14. R. C. HEWITT, S. MEIBOOM, AND L. C. SNYDER, *J. Chem. Phys.* **58,** 5089 (1973).
15. L. C. SNYDER AND S. MEIBOOM, *J. Chem. Phys.* **58,** 5096 (1973).
16. A. PINES, *in* "Proceedings of the 100th Fermi School on Physics" (B. Maraviglia, Ed.), in press.
17. A. PINES, D. J. RUBEN, S. VEGA, AND M. MEHRING, *Phys. Rev. Lett.* **36,** 110 (1976); A. PINES, S. VEGA, AND M. MEHRING, *Phys. Rev. B* **18,** 112 (1978).

18. D. SUWELACK, M. MEHRING, AND A. PINES, *Phys. Rev. B* **19,** 238 (1979).
19. M. GOCHIN, K. V. SCHENKER, H. ZIMMERMAN, AND A. PINES, *J. Am. Chem. Soc.* **108,** 6813 (1986).
20. J. S. WAUGH, *J. Magn. Reson.* **50,** 30 (1982).
21. D. SUTER, K. V. SCHENKER, AND A. PINES, *J. Magn. Reson.* **72,** 90 (1987).
22. U. HAEBERLEN, "High Resolution NMR in Solids, Selective Averaging" *in* "Advances in Magnetic Resonance, Supplement 1" (J. S. Waugh, Ed.), Academic Press, New York, 1976.
23. D. P. BURUM, M. LINDER, AND R. R. ERNST, *J. Magn. Reson.* **44,** 173 (1981).
24. R. TYCKO, H. M. CHO, E. SCHNEIDER, AND A. PINES, *J. Magn. Reson.* **61,** 90 (1985).
25. R. TYCKO, Ph.D. thesis, University of California, 1984.
26. A. J. SHAKA AND A. PINES, *J. Magn. Reson.* **71,** 495 (1987).
27. M. H. LEVITT, D. SUTER, AND R. R. ERNST, *J. Chem. Phys.* **80,** 3064 (1983).
28. R. TYCKO, *Phys. Rev. Lett.* **51,** 775 (1983).
29. R. TYCKO, E. SCHNEIDER, AND A. PINES, *J. Chem. Phys.* **81,** 680 (1984).
30. J. S. WAUGH, *J. Magn. Reson.* **49,** 517 (1982).